

VOYAGER OBSERVATIONS OF MAGNETIC SECTORS AND HELIOSPHERIC CURRENT SHEET CROSSINGS
IN THE OUTER HELIOSPHEREJ. D. RICHARDSON¹, L. F. BURLAGA², J. F. DRAKE³, M. E. HILL⁴, AND M. OPHER⁵¹ Kavli Center for Astrophysics and Space Science, Massachusetts Institute of Technology, Cambridge, 02139, USA; jdr@space.mit.edu² NASA Goddard Space Flight Center, Code 673, Greenbelt, MD 20771, USA; lburlagahsp@verizon.net³ Department of Physics and Institute for Physical Science and Technology, University of Maryland, College Park, MD 20742, USA; drake@umd.edu⁴ Applied Physics Laboratory, The Johns Hopkins University, Laurel, MD 20723, USA; Matthew.Hill@jhuapl.edu⁵ Astronomy Department, Boston University, 675 Commonwealth Avenue, Boston, MA 02215, USA; mopher@bu.edu

Received 2016 May 27; revised 2016 August 24; accepted 2016 August 26; published 2016 November 3

ABSTRACT

Voyager 1 (V1) has passed through the heliosheath and is in the local interstellar medium. *Voyager 2* (V2) has been in the heliosheath since 2007. The role of reconnection in the heliosheath is under debate; compression of the heliospheric current sheets (HCS) in the heliosheath could lead to rapid reconnection and a reconfiguration of the magnetic field topology. This paper compares the expected and actual amounts of time the *Voyager* spacecraft observe each magnetic sector and the number of HCS crossings. The predicted and observed values generally agree well. One exception is at *Voyager 1* in 2008 and 2009, where the distribution of sectors is more equal than expected and the number of HCS crossings is small. Two other exceptions are at V1 in 2011–2012 and at V2 in 2012, when the spacecraft are in the opposite magnetic sector less than expected and see fewer HCS crossings than expected. These features are consistent with those predicted for reconnection, and consequently searches for other reconnection signatures should focus on these times.

Key words: magnetic reconnection – solar wind – Sun: heliosphere

1. INTRODUCTION

In mid-2016 *Voyager 2* (V2) was at 111 AU and had traversed 27 AU of the heliosheath. *Voyager 1* (V1) crossed the heliopause (HP) in 2012 at 124 AU and is now in the local interstellar medium. The solar magnetic field is carried outward through the heliosphere by the solar wind. As described by Parker (1963), B_R decreases in strength as R^{-2} and B_T as R^{-1} , so that the Parker spiral angle approaches 90° and the magnetic field decreases as R^{-1} in the outer heliosphere. *Voyager* observations are consistent with these predictions (Richardson & Burlaga 2013). The solar magnetic field is tilted with respect to the spin axis; the tilt angle varies over a solar cycle and is lowest at solar minimum and largest at solar maximum (<http://wso.stanford.edu/>). The heliospheric current sheet (HCS) separates regions where the magnetic field lines point in the direction leading toward the Sun (toward sectors) and leading away from the Sun (away sectors) (Ness & Burlaga 2001; Burlaga et al. 2003). The latitudes comprising the sector zone, the region in which HCS crossings are observed (Burlaga & Ness 1993), are determined by the solar magnetic tilt and the meridional flow (which is important only in the heliosheath). To first order, for a tilt angle of 30° HCS crossings are observed at heliolatitudes up to $\pm 30^\circ$ (latitudinal symmetry is not required). The tilt angles are calculated at the Wilcox Solar Observatory (WSO) by applying two potential models to photospheric magnetic field observations (<http://wso.stanford.edu/>). The classic model is preferred and uses a line-of-sight boundary condition at the photosphere. The classic model does a good job (better than the radial model) of reproducing *Voyager* HCS locations in the outer heliosphere (Burlaga & Ness 1997). Pogorelov et al. (2014) show that the extent of the HCS in the heliosheath depends on the velocity vector and always extends to high latitudes near the HP.

When the *Voyagers* crossed the termination shock (TS), the magnetic field magnitude increased by a factor of roughly 2

(Burlaga et al. 2005, 2008), the plasma speed slowed by a factor of 2, and the flow velocity gained a component directed roughly away from the nose of the heliosphere (Richardson et al. 2008). The radial plasma flow decreases across the heliosheath; the slower and more variable heliosheath flows cause the HCS crossings to be distorted and compressed. Several authors suggest that reconnection occurs in the “sector” region of the heliosheath where HCS crossings are compressed (Lazarian & Opher 2009; Drake et al. 2010) and that the outer heliosheath could be a region of magnetic bubbles (Opher et al. 2011). This scenario could help explain the very different energetic particle (especially electron) intensities observed at V1 and V2 (Hill et al. 2014) and the lack of conservation of magnetic flux observed at V1 (Richardson et al. 2013). Observationally, the magnetic bubble boundaries can be difficult to differentiate from standard HCS crossings. Recent models suggest that continued reconnection may drastically reduce the number of HCS crossings observed as magnetic regions merge at the high-latitude edges of the sector regions where regions of one polarity are much wider than regions of the other. J. F. Drake et al. (2016, in preparation) suggest that the thinner polarity regions are annihilated by reconnection, which results in the formation of large regions with a single sector and few HCS crossings. Other mechanisms such as turbulence could also change the sector structure.

This paper compares the percentages of toward and away magnetic polarity sectors observed versus those predicted. We also present the number of HCS crossings observed each year in the outer heliosphere and heliosheath. We then discuss these results in the context of the reconnection hypotheses.

2. THE DATA

Magnetic field data are obtained from two independent magnetometers on each *Voyager* spacecraft (Behannon et al. 1977). These data are used to determine B_R , B_T , and

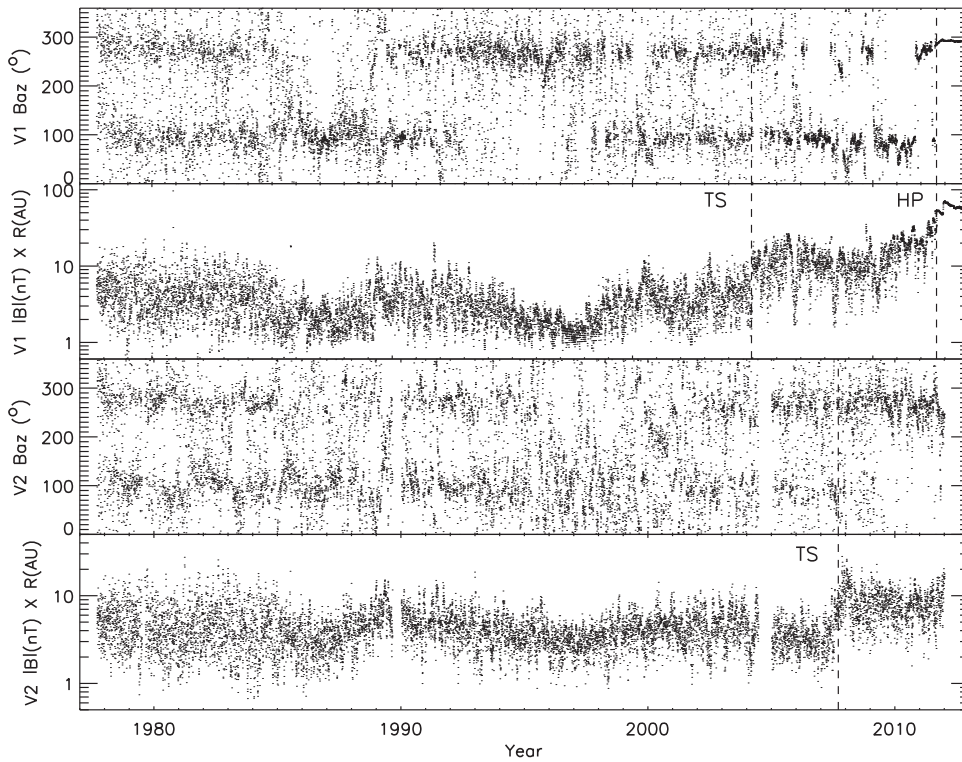


Figure 1. Daily averages of the azimuthal angle B_{az} and magnetic field magnitude from *V1* and *V2* observations. B_{az} is in the RT plane, is zero in the radial direction and increases in a clockwise direction.

B_N , although uncertainties are introduced by the relatively large spacecraft magnetic field. The magnetic field analysis and uncertainties are described in detail by the *Voyager* magnetometer team (Burlaga et al. 2016). In this work, we use the 1 day average magnetic field values from NASA’s Space Physics Data Facility web site (spdf.gsfc.nasa.gov).

The *V2* plasma velocities are derived from measurements from the four modulated-grid Faraday cups on the plasma experiment (Bridge et al. 1977). The observed current versus energy spectra are fitted assuming convected isotropic Maxwellian proton distributions. These distributions fit the data well with uncertainties in V_R of about 10% and in V_T and V_N of 30 km s^{-1} (Richardson & Decker 2014). The daily averages used in this study are archived at <http://web.mit.edu/space/www/voyager.html>. The *V1* plasma instrument does not work, so consequently the *V1* velocity components used in this work are derived from energetic particle observations from the LECP and CRS instruments using the Compton–Getting effect (Decker et al. 2012; Stone & Cummings 2012).

Figure 1 shows the daily average magnetic field azimuthal angles (B_{az}) and magnitudes for *V1* and *V2*. The bifurcated nature of the B_{az} angles is obvious; the most frequently observed directions are 90° and 270° . At the solar minima in 1986 and 1996, *V1* observes mainly one sector as the tilt of the current sheet is comparable to the *V1* heliolatitude. *V2* observes this effect to a lesser degree in 1996. At *V1* distinct sectors are observed across the heliosheath, whereas at *V2* after 2009 most angles are near 270° . The elevation angles (not shown) are centered on zero with a large spread. The magnitudes clearly show the solar cycle variation with stronger fields near solar maxima. The magnetic field magnitudes increase at the TS and HP.

Figure 2 shows the *V1* and *V2* heliolatitudes and the WSO tilts derived using the classic model for northern and southern heliolatitudes. *V1* moved north of the equator after the Saturn encounter in 1980. *V2* stayed near the equator until after the Neptune encounter in 1990 at 30 AU when it was deflected southward. When the spacecraft heliolatitudes are less than the HCS tilt, the spacecraft are in the sector zone and should observe both magnetic field polarities. When the spacecraft heliolatitudes are greater than the HCS tilts, then the spacecraft should be in the unipolar zone and observe only one magnetic polarity. During the solar minima in 1986, 1996, and 2008 *V1* should be in the unipolar region for well over a year. *V2* is never expected to be in the unipolar region for long periods. The sector structure propagates outward with the solar wind, so that there is a delay in the effects of the HCS tilt arriving at the *Voyager* spacecraft, which is small near the Sun, but over a year in the heliosheath. This plot does not correct for the propagation time.

The lower panel of Figure 2 shows the fraction of days *V1* and *V2* spent in the away sector in each year. These fractions are calculated using the daily averages of the magnetic field angles. A day is defined to be in the away sector if B_{az} is 210° – 330° (within 60° of the nominal Parker angle at large distances) and in the toward sector if B_{az} is 30° – 150° . Days with angles outside these ranges are not included; the fractions shown are the number of days each year *V1* or *V2* are in the away sector divided by the total number of days in that year that the spacecraft are in either the toward or away sectors.

The plot shows roughly the expected relationship. *V1* observed over 90% away sectors in 1986–1988 when it was above the HCS tilt, over 90% toward sectors in 1995–1996 when it was again above the HCS (but the solar field had reversed), and large percentages of away field in the

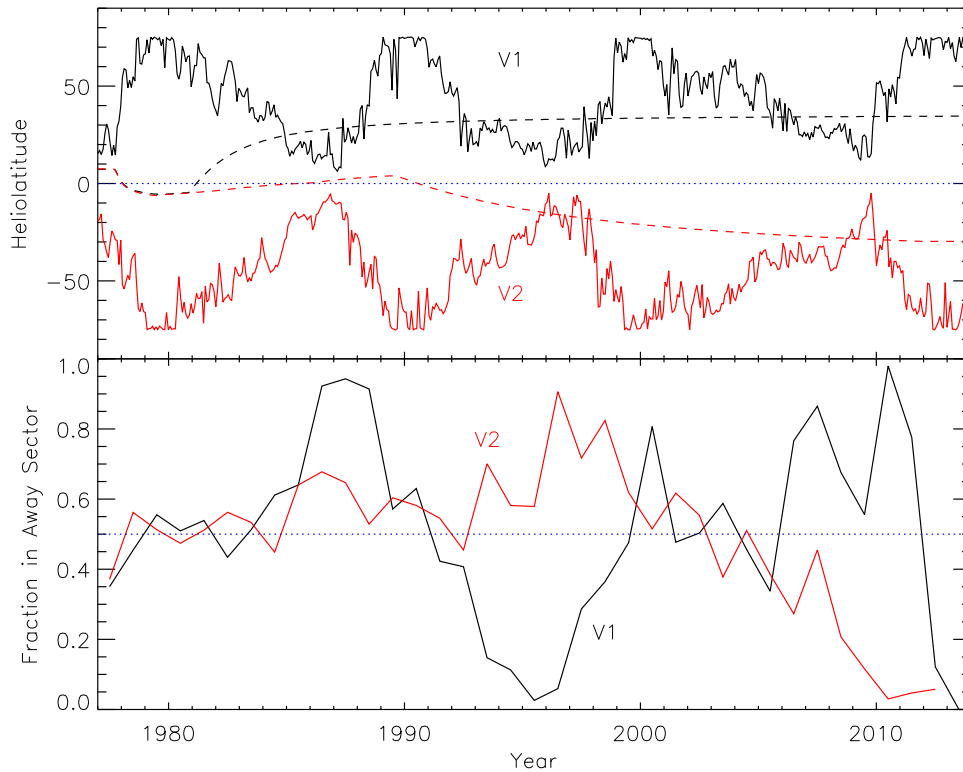


Figure 2. The top panel shows the tilt of the HCS from the WSO classic model for the northern (black) and southern (red) hemispheres. The dashed lines show the $V1$ and $V2$ heliolatitudes and the dotted blue line shows the equator. The bottom panel shows the fraction of the time $V1$ and $V2$ are in the away magnetic sector of the solar wind. The dotted blue line shows the 50% location.

2006–2011 minimum. When the tilts are large near solar maxima, the toward and away sector percentages are similar. $V2$ was in the away sector more often in 1996–1998 when it was near the edge of the sector region and in the toward region more often from 2009–2012.

Figure 3 shows a quantitative comparison of the expected versus observed time in each sector. To make the comparison more easily visible, instead of showing toward and away sectors, which reverse every solar maximum, for $V1$ we show the observed fraction of days in the southern sector. For $V2$, we show the fraction observed in the opposite heliolatitude to which the spacecraft is in, which is primarily in the north. The expected fractions spent in each sector by $V1$ and $V2$ are calculated using the WSO tilts for each hemisphere assuming a sinusoidal oscillation of the HCS as the Sun rotates. We assume the average solar wind speed in each sector is the same. The blue line in Figure 3 shows the results for the radial WSO model and the black line shows the classic model.

We again note the the WSO HCS tilts are for data at the Sun. The sectors take an increasing amount of time to propagate to the *Voyager* spacecraft. As a rough estimate, for this plot we assumed a 360 day transit time to 90 AU ($V_R = 430 \text{ km s}^{-1}$) and timeshifted the data accordingly. We did not attempt to correct further for the slower heliosheath speeds since for the 1 year time segments of data used here small timeshifts are not important.

The observed fraction of time in each sector is given by the red line in each panel. We add one more complication. In the supersonic solar wind the flow is observed to be essentially radial (although models show stream interactions could produce some V_N ; Borovikov et al. 2012), and consequently the HCS is carried radially outward with the flow. In the

heliosheath the flow is deflected; northward and southward flows change the latitudinal extent of the HCS. Northward flow is observed at $V1$ and southward flow at $V2$, so that at both spacecraft flow is away from the equator and enlarges the latitudinal width of the sector region. The *Voyager* observations of V_N are used to calculate the change in the sector region latitudinal width; at $V1$ the meridional flow angle is about 45°N and at $V2$ it averages about 20°S (Stone & Cummings 2012; Richardson & Decker 2014). The full latitudinal velocity profile is not measured, and so we use the local *Voyager* observations to represent the flows throughout the sector region. $V2$ samples V_R and V_N in and out of the sector zone and no systematic change in RN flow angle is observed with distance from the HCS, and consequently this assumption seems reasonable. The green lines in Figure 3 show the expected fraction in each sector when V_N in the heliosheath is accounted for; for $V1$ the fraction increases by up to 0.1 but for $V2$ there is little effect.

Figure 3 shows a generally good agreement between the expected and observed fractions of time in each sector. Consistent with past results, the classic model matches the data better than the radial model. For $V1$ the observed fraction in the southern sector tracks the prediction well, but tends to be slightly higher than predicted. At solar maxima this difference is likely because the WSO models are not accurate for tilts over 70° . At solar minima more of the southern sector is observed than expected, but the differences are generally less than 10% and could result from solar wind dynamics. For example, poleward flows have been reported at solar minima (Richardson & Paularena 1996; Burlaga & Richardson 2000), which would widen the sector region. For $V2$ the observations and

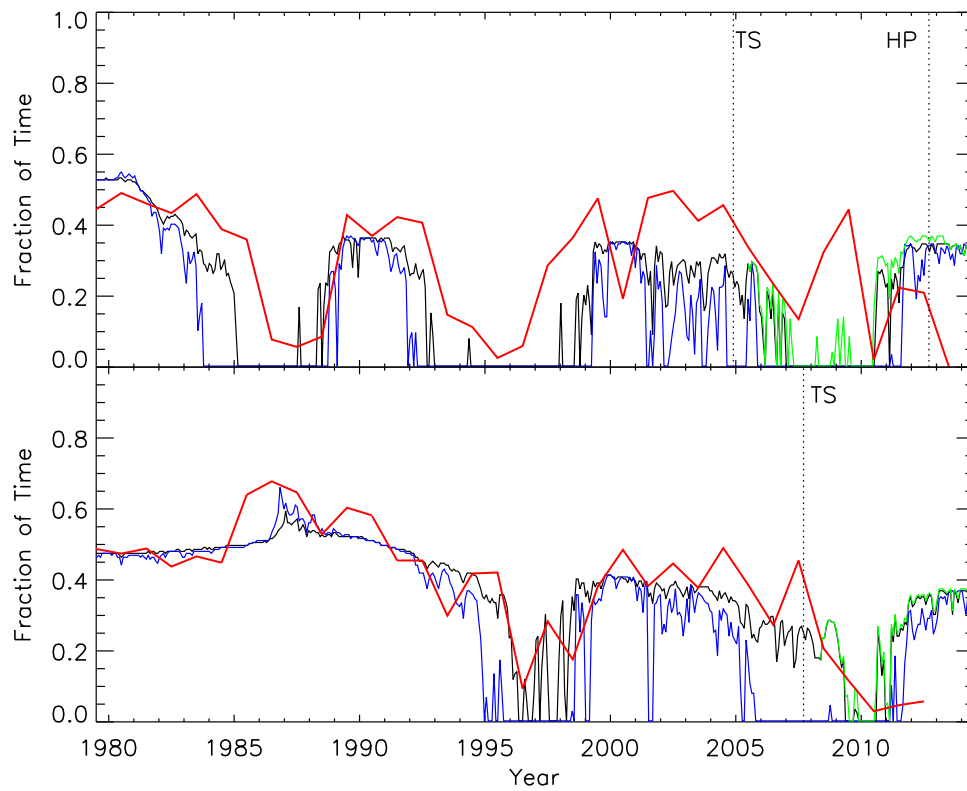


Figure 3. The top panel shows $V1$ and bottom panel $V2$. The red lines are the fraction of days observed with B_{az} in the sector opposite the spacecraft heliolatitude (so when $V1$ is at northerly latitudes, the fraction of days in the southern sector). The blue line is the predicted fraction using the WSO radial model, the black line the predicted fraction using the WSO classic model, and the green line the predicted fraction using the WSO classic model with the sector region expanding due to the measured V_N in the heliosheath. These model fractions are timeshifted using an average speed of 430 km s^{-1} . The TS and HP locations are shown by the dotted lines.

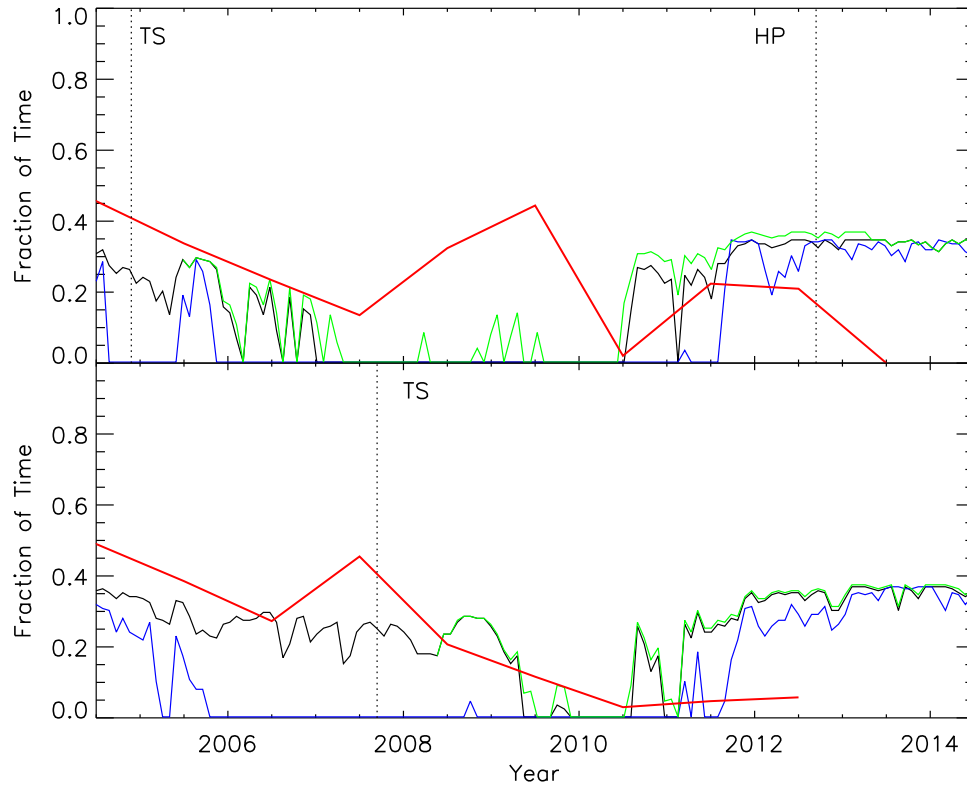


Figure 4. Same as Figure 3 with the heliosheath region expanded.

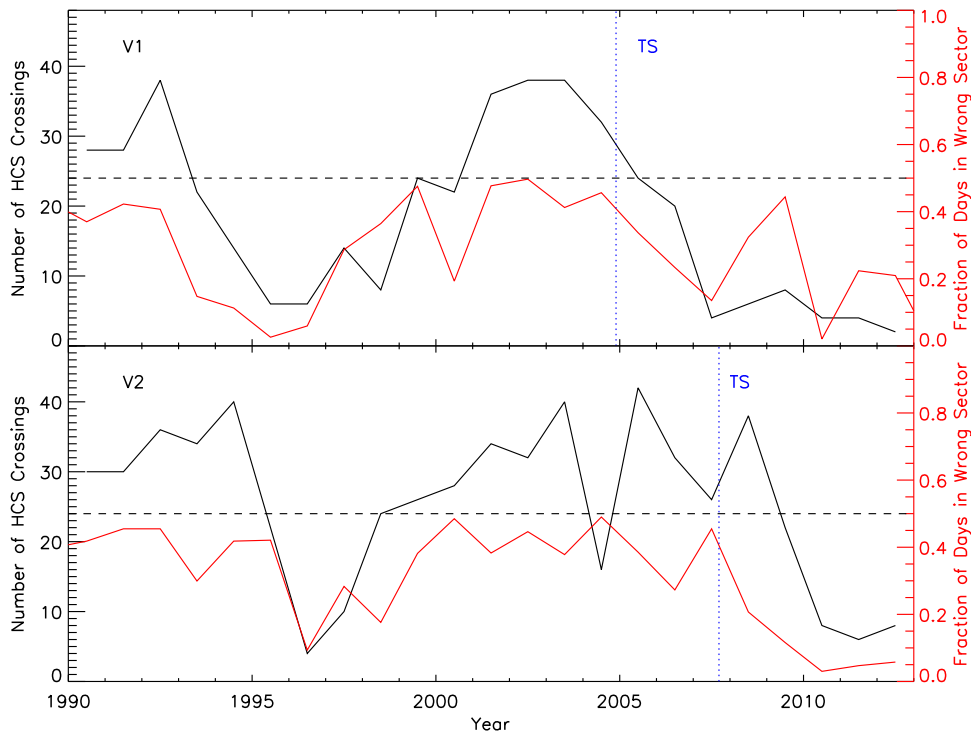


Figure 5. The top panel shows *V1* and bottom panel *V2*. The black line shows the number of HCS crossings each year. The red lines show the fraction of days with the magnetic field in the opposite sector. The dotted lines show the TS locations and the dashed lines where the fraction is 50%.

predictions based on the WSO classic model agree well in the solar wind up to 2012.

Figure 4 shows a blow-up of Figure 3 focusing on the heliosheath where reconnection is hypothesized to be important. The biggest discrepancy between the expected and observed fractions at *V1* is from 2008–2010 when 40% southern polarity is observed compared to only 10% expected. This observation is opposite the expected reconnection signature. However, we note that in this region of the heliosheath *V1* observed a decrease in V_R from 50 km s^{-1} at 2008.0 to 0 at 2010.4 and entered the stagnation region (Krimigis et al. 2011). The physics of this region are not well understood but the unexpected flows may result from transient effects, which could effect the heliosheath morphology (Pogorelov et al. 2012). In 2011 and 2012 the *V1* observed fraction of opposite polarity is lower than predicted. For *V2* the only major discrepancy between the expected and observed polarity fraction is in 2012 when the observed fraction of opposite polarity is significantly less than that predicted. These 2011–2012 *V1* and 2012 *V2* signatures are those predicted for reconnection. When more *V2* magnetic field data are available, we will see if this signature persists.

Another predicted signature of reconnection in the heliosheath is a change in the number of HCS crossings, coincident with a change in the fraction of time spent in each sector. Reconnection in the heliosheath could produce large regions with the same magnetic polarity and few HCS crossings in the high-latitude sector zone (J. F. Drake et al. 2016, in preparation). This hypothesis is tested by looking at the number of HCS crossings observed at *V1* and *V2* in the outer heliosphere and heliosheath. HCS crossings were picked by hand. Crossings based on a single point were not included, nor were events which did not have clear, large, and rapid direction changes. The number of expected crossings depends

on the solar magnetic field configuration. At solar minima the solar field is largely dipolar, so that we expect to see two HCS crossings per solar rotation at the solar equator, or about 28 each year. At solar maxima the field is highly complex, often resulting in four or more HCS crossings per solar rotation. Since the *Voyagers* move radially outward the expected numbers are slightly reduced, by the ratio of the solar wind radial speed to the spacecraft speed, or about 4% in the solar wind and 17% in the heliosheath for *V2*. Figure 5 shows the number of HCS crossings each year at *V1* and *V2* and the fraction of the year when *V1* and *V2* are in the opposite polarity region. In the 1996 solar minimum, when *V1* and *V2* were in the supersonic solar wind, the number of HCS crossings at each spacecraft is less than ten. Both spacecraft primarily remain in one sector. After the 1990 and 2000 solar maxima HCS crossings are common, up to 40 per year, as expected. About 2 years after crossing the TS, both *V1* and *V2* see a large decrease in the number of HCS crossings. After 2005 for *V1* and 2011 for *V2*, the number of HCS crossings is less than ten. For *V2* the fraction of time spent in the opposite sector is also small, so that it is likely above the sector zone. For *V1*, however, the number of HCS crossings is low in 2008 and 2009 even though it is in the wrong sector about 40% of the time. We expect the number to be smaller than normal, because of the slow V_R observed at *V1* as it approached the stagnation region. The average V_R from 2008 was 35 km s^{-1} and for 2009 was 25 km s^{-1} . Since the spacecraft speed is 17 km s^{-1} , this effect would reduce the expected number of crossings to about 14 in 2008 and nine in 2009, which is still more than observed.

The hypothesis being tested is whether or not the number of HCS crossings is less than expected in the heliosheath at the times where reconnection signatures may be present. These time periods are 2011–2012 for *V1* and 2012 for *V2*. In both of these time periods the number of HCS crossings is less than

ten, which would be consistent with the reconnection hypothesis. However, the low number of HCS crossings at *VI* could result from its location in a region where the radial flow is comparable to the spacecraft speed, which could cause it to remain in the same sector for long periods of time. *V2* should be well inside the sector zone and observes a radial speed of about 90 km s^{-1} in 2012, and consequently should have more HCS crossings than observed.

3. SUMMARY

The role of reconnection in the heliosheath is under debate. The consequences of reconnection may depend on location within the sector zone. In the middle of the zone, where toward and away polarity regions are similar in radial width, magnetic bubbles may form, which are difficult to distinguish from normal HCS crossings. At the high-latitude edges of the sector zone, where one polarity region is much wider than the other, the sectors in the heliosheath may merge, forming large regions of a single polarity. We look at the observed sector structure and HCS crossings for evidence of the latter effect. We find that the fraction of time spent in each sector generally, but not always, agrees with that predicted based on the WSO-derived HCS tilt angles and observed flow angles in the supersonic solar wind. The agreement is better for *V2* than *VI*. At *VI* the fractions of toward and away sectors are generally more equal than predicted by about 0.1. In the heliosheath, the biggest discrepancy is for *VI* in 2008 and 2009 where the prediction is for less than 10% toward polarity, but about 40% is observed. The number of HCS crossings generally varies as expected, again with the exception of at *VI* in 2008 and 2009; in those two years the fractions of toward and away sectors is comparable, but very few (<10) HCS crossings are observed. The times when the data may be consistent with the reconnection hypothesis are for *VI* in 2011 and 2012 and *V2* in 2012, when the magnetic field is more unipolar than expected and the number of HCS crossings less than predicted. When *V2* magnetic field data from more recent years are available, the role of reconnection in the heliosheath should be clarified.

We wish to acknowledge support from the International Space Science Institute for the team “Facing the Most Pressing

Challenges to Our Understanding of the Heliosheath and its Outer Boundaries”, which spurred this work and we thank WSO for providing the HCS data. JDR was supported under NASA contract 959203 from the Jet Propulsion Laboratory at the Massachusetts Institute of Technology. L. F. Burlaga was supported by NASA Contract NNG14PN24P. M. O. acknowledges the support of NASA Grand Challenge NNX14AIB0G and NASA award NNX13AE04G. J.D.F. was supported by NASA grant NNX14AF42G.

REFERENCES

- Behannon, K. W., Acuna, M. H., Burlaga, L. F., et al. 1977, *SSRv*, **21**, 235
 Borovikov, S. N., Pogorelov, N. V., & Ebert, R. W. 2012, *ApJ*, **750**, 42
 Bridge, H. S., Belcher, J. W., Butler, R. J., et al. 1977, *SSRv*, **21**, 259
 Burlaga, L. F., & Ness, N. F. 1993, *JGR*, **98**, 17415
 Burlaga, L. F., & Ness, N. F. 1997, *JGR*, **102**, 19731
 Burlaga, L. F., Ness, N. F., Acuña, M. H., et al. 2005, *Sci*, **309**, 2027
 Burlaga, L. F., Ness, N. F., Acuña, M. H., et al. 2008, *Natur*, **454**, 75
 Burlaga, L. F., Ness, N. F., & Richardson, J. D. 2003, *JGR*, **108**, 8028
 Burlaga, L. F., Ness, N. F., Richardson, J. D., Decker, R. B., & Krimigis, S. M. 2016, *ApJ*, **818**, 147
 Burlaga, L. F., & Richardson, J. D. 2000, *JGR*, **105**, 10501
 Decker, R. B., Krimigis, S. M., Roelof, E. C., & Hill, M. E. 2012, *Natur*, **489**, 124
 Drake, J. F., Opher, M., Swisdack, M., & Chamoun, J. N. 2010, *ApJ*, **709**, 963
 Hill, M. E., Decker, R. B., Brown, L. E., et al. 2014, *ApJ*, **781**, 94
 Krimigis, S. M., Roelof, E. C., Decker, R. B., & Hill, M. E. 2011, *Natur*, **474**, 359
 Lazarian, A., & Opher, M. 2009, *ApJ*, **703**, 8
 Ness, N. F., & Burlaga, L. F. 2001, *JGR*, **106**, 15803
 Opher, M., Drake, J. F., Swisdack, M., et al. 2011, *ApJ*, **734**, 71
 Parker, E. N. 1963, *Interplanetary Dynamical Process*, Interscience Publishers (New York: Wiley)
 Pogorelov, N. V., Borovikov, S. N., Heerikhuisen, J., Kim, T. K., & Zank, G. P. 2014, in *ASP Conf. Ser. 488, 8th Int. Conf. of Numerical Modeling of Space Plasma Flows (ASTRONUM 2013)*, ed. N. V. Pogorelov, E. Audit, & G. P. Zank (San Francisco, CA: ASP), 167
 Pogorelov, N. V., Borovikov, S. N., Zank, G. P., Burlaga, L. F., & Decker, R. B. 2012, *ApJL*, **750**, L4
 Richardson, J. D., & Burlaga, L. F. 2013, *SSRv*, **176**, 217
 Richardson, J. D., Burlaga, L. F., Decker, R. B., et al. 2013, *ApJL*, **762**, L14
 Richardson, J. D., & Decker, R. B. 2014, *ApJ*, **792**, 126
 Richardson, J. D., Kasper, J. C., Wang, C., Belcher, J. W., & Lazarus, A. J. 2008, *Natur*, **464**, 63
 Richardson, J. D., & Paularena, K. I. 1996, *JGR*, **101**, 19995
 Stone, E. C., & Cummings, A. C. 2012, *Proc. ICRC (Beijing)*, **12**, 23